

Analysis of influencing factors on the achievability of bistable fully closed shells by semi-analytical modelling

Pavlo Pavliuchenko^{1*}, Marco Teller¹, Gerhard Hirt¹

¹Institute of Metal Forming (IBF), RWTH Aachen University, 52072 Aachen, Germany

*Corresponding author.

Abstract

Bistable fully closed shells can serve as long supporting structures that can be folded into a compact transport geometry and unfolded at the construction place. Bistability is achieved by introducing a specific distribution of residual stresses through the thickness of the shell, e.g. by incremental die-bending. In order to find a suitable bending radii combination a semi-analytical model was developed and experimentally validated for the steel 1.1274 in previous research. Nevertheless, minor deviations have occurred in the prediction of final curvatures of the different stable geometries and it is still unclear to what extent other influencing variables such as shell thickness or material properties influence the achievability of fully closed bistable shells. Therefore, in this paper, an enhancement and generalization of the existing semi-analytical model for different steels is described and the extended model is used for a comprehensive analysis of the influence of different variables on bistability and final shell geometries.

Keywords: *bistability, residual stress, sheet metal*

1 Introduction

Deployable structures can be defined as structures that have two main stable states, namely a compact and a deployed geometry [1]. The compact state is mainly used for transportation and therefore should occupy the smallest possible volume. Additionally, a housing is necessary to keep the structure in the compact state. In contrast, bistable structures are deployable structures that have stable geometries in both states [1]. Such structures could be produced from metallic thin shells with high yield strength by introducing a specific residual stress distribution over the shell thickness [2]. The general production route of bistable metallic shells was described in [3] and consists of two sequential plastic bending steps in opposite directions, along two orthogonal axes (see Fig. 1). The particular residual stress distribution over the shell thickness, introduced during the bending process, provides two stable states, as shown in Fig. 2, where X- and Y-axis represent the longitudinal and transverse directions. The Z axis represents the thickness of the shell and is not shown in the figure, since due to the small thickness the stresses in this direction are not considered.

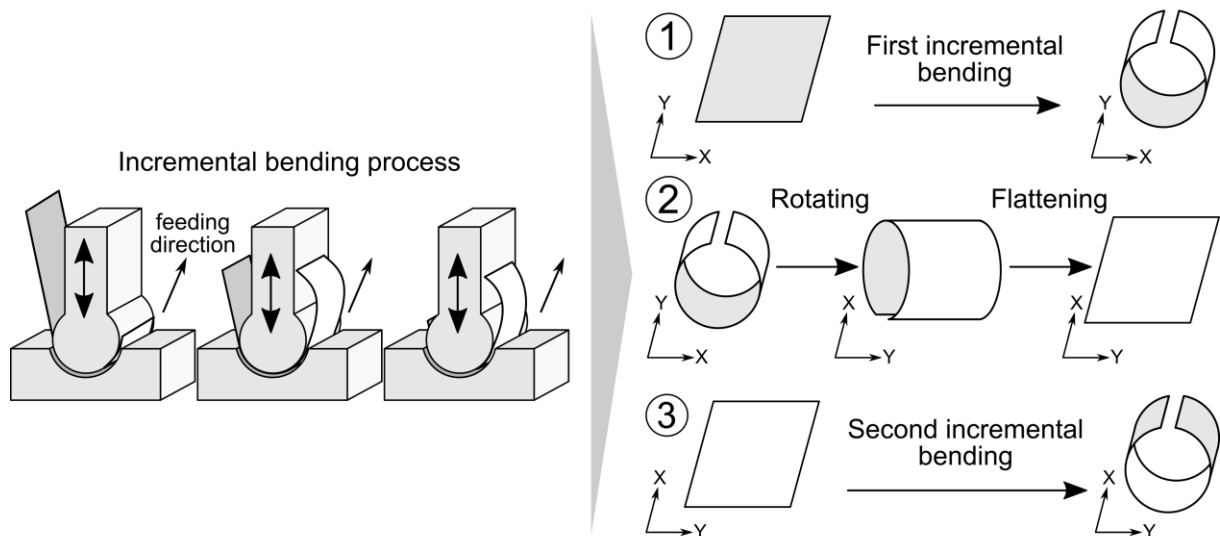


Fig. 1: Scheme of the production process of bistable shells [3]

The analytical models for determination the effect of bistability of such structures are given by Galletly and Guest using beam [4] and shell [5] models and He [6], respectively. In [7], a semi-analytical model for the rapid determination of possible bending radii combinations was developed. This model works with some simplifications and assumptions, which are only valid for the steel 1.1274 used in [7]. In order to enable the investigation of various influencing factors and to allow for a general investigation on the influences on bistability, the model is firstly extended in this paper. Afterwards, a comprehensive study of a wide range of parameters is presented. This large number of simulations can only be performed due to the fast computing time (less than 3 s per simulation) of the semi-analytical model.

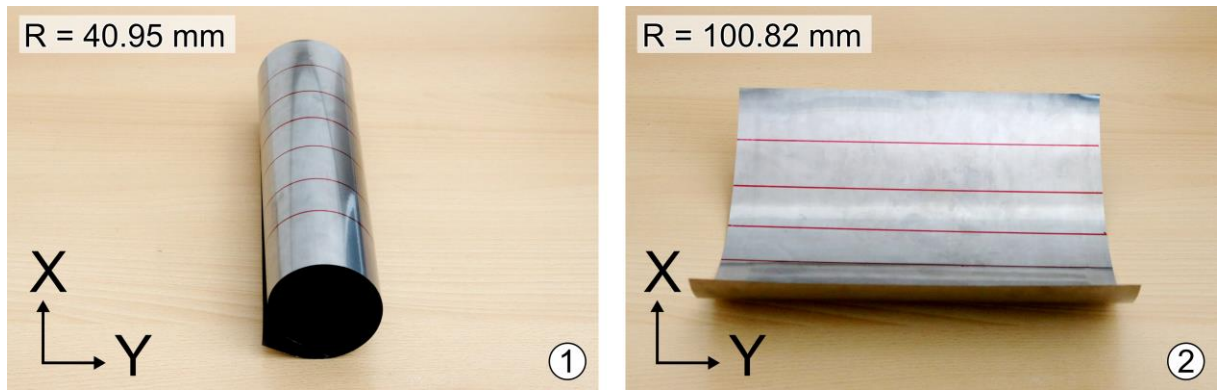


Fig. 2: Bistable tube produced by incremental bending (1: deployed state as the first stable state, 2: (partially) folded configuration as the second stable state). [3]

2 Semi-analytical model

2.1 Model extension and generalization

The semi-analytical model for investigation of the influence of production process parameters on bistable shells for the steel 1.1274 was introduced in [3]. The production process described by this model could be represented by the sequence of following steps: first bending of the shell along X-axis; flattening of the shell; second bending of the shell along Y-axis in opposite direction; springback to the first stable state; flattening of the shell and slight bending of it along X-axis in order to check second stable state.

As already mentioned, some assumptions were made specifically for the material 1.1274 used. A main assumption is, that during the first bending process only kinematic hardening and during the second bending only isotropic hardening occurs, respectively. A general combined hardening approach, where both, kinematic and isotropic hardening, contribute to the plastic behavior of the material, seems to be suitable. Hence, a combined isotropic/kinematic hardening behavior during first and second bending was introduced into the new model.

In the original model, the thickness of the shell was divided into an elastic part, where only elastic deformation occurs, and a plastic part, where plastic hardening takes place. Both parts were afterwards divided into an equal number of layers. This approach could lead to different layer thickness in elastic and plastic parts of shell, which may affect the accuracy of calculations. Also, the initial division of the shell on elastic and plastic regions leads to difficulties in calculation the second bending step, where the ratio of these regions may differ in comparison with the first bending. To avoid complications, in the new model the shell thickness is initially divided into 100 layers with equal thickness and then stresses are calculated for each layer. An initial splitting into elastic and plastic areas no longer takes place.

2.2 Extended Semi-analytical model

Based on the semi-analytical model described in [7] several changes were made. A combined isotropic/kinematic hardening model was introduced. During plastic deformation the yield locus translates (kinematic part) as well as increases in size (isotropic part). The ratio of kinematic and isotropic hardening on the total hardening of the shell is assumed to be 0.5 [8]. Also, the shell thickness is divided by 100 layers with equal size.

In order to avoid unnecessary repetition of the work in [7], here only the most important equations and changes compared to the former model will be described.

The strain along the bending direction is described by the multiplication of shell curvature k and layer thickness z and provided in equation (1):

$$\varepsilon = k \cdot z \quad (1)$$

The elastic stress calculation is presented in equation (2):

$$\sigma = E \varepsilon_e = E(\varepsilon - \varepsilon_p) \quad (2)$$

where E is the Young's modulus of the material.

The elastic stress increment is shown in equation (3):

$$d\sigma = C d\varepsilon_e \quad (3)$$

where C is the stiffness matrix defined as:

$$C = \frac{E}{1-\nu^2} \begin{bmatrix} 1 & \nu \\ \nu & 1 \end{bmatrix} \quad (4)$$

where ν is Poisson's ratio.

The equivalent stress is presented in equation (5):

$$\sigma_e = \frac{1}{\sqrt{2}} \sqrt{(\sigma - X)^T A (\sigma - X)} \quad (5)$$

where X is the so called back stress, and its increment could be calculated by equation (6):

$$dX = \frac{c}{\sigma_{y0}}(\sigma - X)dp - \gamma X dp \quad (6)$$

The isotropic hardening plastic stress increment is calculated via equation (7):

$$d\sigma = C \left(I - \frac{a \cdot C \cdot a}{a \cdot C \cdot a + b Q e^{-bp}} \right) d\varepsilon \quad (7)$$

and the kinematic hardening plastic stress increment is presented in equation (8):

$$d\sigma = C \left(I - \frac{a \cdot C \cdot a}{a \cdot C \cdot a - \left(\gamma + \frac{c}{\sigma_{y0}} \right) a \cdot X + \frac{c}{\sigma_{y0}} \sigma \cdot a} \right) d\varepsilon \quad (8)$$

where a is the normal to the yield locus, I is identity matrix and γ , c , b , Q are material flow curve constants. The weighting of the two hardening mechanisms is determined by the parameter m . The combined strain rate is presented in equation (9) [8]:

$$\dot{\varepsilon}_p = \dot{\varepsilon}_{pi} + \dot{\varepsilon}_{pk} = m\dot{\varepsilon}_p + (1 - m)\dot{\varepsilon}_p \quad (9)$$

Combining equations (7) and (8) the plastic stress increment for the combined hardening model is given by equation (10):

$$d\sigma = C \left(I - \frac{a \cdot C \cdot a}{a \cdot C \cdot a - (1-m) \left(\left(\gamma + \frac{c}{\sigma_e} \right) a \cdot X - \frac{c}{\sigma_e} \sigma \cdot a \right) + mb Q e^{-mbp}} \right) d\varepsilon \quad (10)$$

where at parameter $m=0$ pure kinematic hardening and at $m=1$ pure isotropic hardening occurs during the plastic deformation of the material.

When considering the stability of shell geometry after springback, it is assumed that the resulting bending moment inside the shell is equal to zero. Due to the symmetry about the mid-surface, the integrated, applied bending moment through the thickness can be calculated as

$$M = 2 \int_0^{T/2} \sigma(z) z dz \quad (11)$$

where T is the thickness of shell.

The shell geometry is considered stable if the resulting bending moment per unit length for the required axis is close to zero. Based on the study [9], the applied bending moment per unit length (M) and curvature (k) has a linear relationship during elastic unloading. The slope of this elastic recovery is given by equation (12):

$$\frac{M}{k} = \frac{2 E (T/2)^3}{3 (1-\nu^2)} \quad (12)$$

As the bending moment after spring back should be zero, then the curvature after spring back, k_{sp} , can be derived from Equation (12) as

$$k_{sp} = k_x - \frac{3(1-\nu^2)M}{2E(T/2)^3} \quad (13)$$

where k_x is the first bending curvature.

3 Materials

For the parameter studies the steels 1.1274 and 1.4310 were used. The main difference between these materials is the yield strength. The stress-strain curves and material constants are provided in Fig. 3 and Table 1, respectively. The shell thickness is 0.2 mm for both materials.

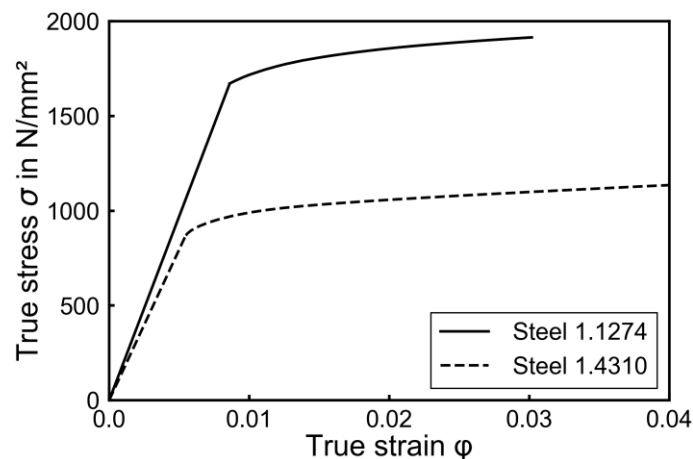


Fig. 3: Stress-strain curves of steels 1.1274 and 1.4310.

Table 1: Material property constants

Steel	σ	E	c	γ	b	Q
1.1274	1690 MPa	189450 MPa	33933	152.576	152.576	222.403
1.4310	918 MPa	158920 MPa	30520	194.284	194.284	157.089

3.1 Choosing appropriate m-value

In order to find the appropriate ratio between kinematic and isotropic parts of combined hardening the evaluation of experimental data was done. For this reason, the comparison between experimentally obtained springback shell radii after first second bending for the steel 1.1274 was carried out and the results are given in Fig. 4. It can be seen of the graph, that, for all bending radii R_{bend} , shell radius after elastic springback after second bending (bending of pre-bent shell) is always smaller than shell radius after first bending of the flat shell.

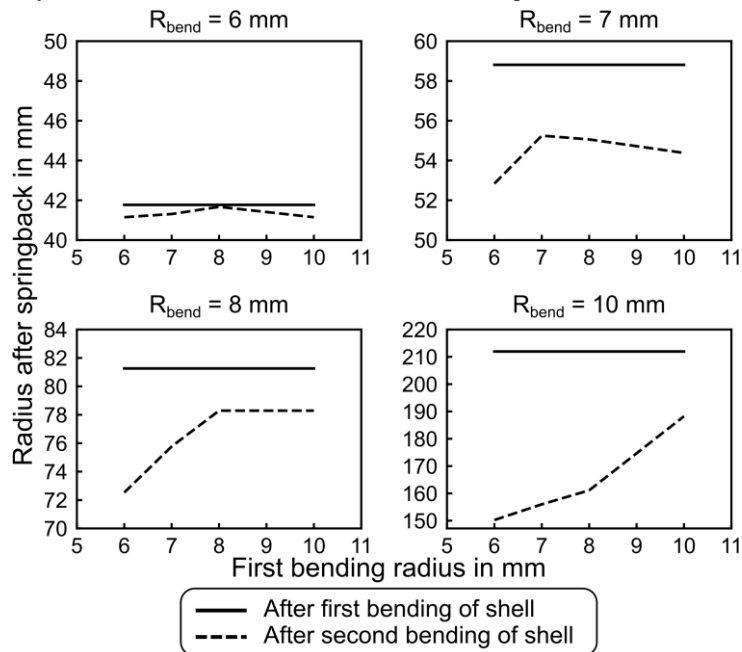


Fig. 4: Experimentally obtained shell radii after elastic springback after first and second bending of the shell.

To determine which m -value should be used during parameter study, the comparison of springback shell radii for different m -value after first and second bending using semi-analytical model was carried out. The results are presented in Fig. 5. For a bend radius R_{bend} of 10 mm, the results are not presented, because a stable geometry after the second bending was not achieved. As can be seen, with increasing the isotropic part in the combined hardening (m approaches 1), the calculated shell radius after second springback became greater than after first bending. This difference is minimal when the pure kinematic hardening is considered during plastic deformation. It should be mentioned, that even for the pure kinematic hardening the calculated shell radius after second springback is not always greater than after first bending. Therefore, the pure kinematic hardening ($m = 0$) was chosen to perform the parameter study by the help of semi-analytical model.

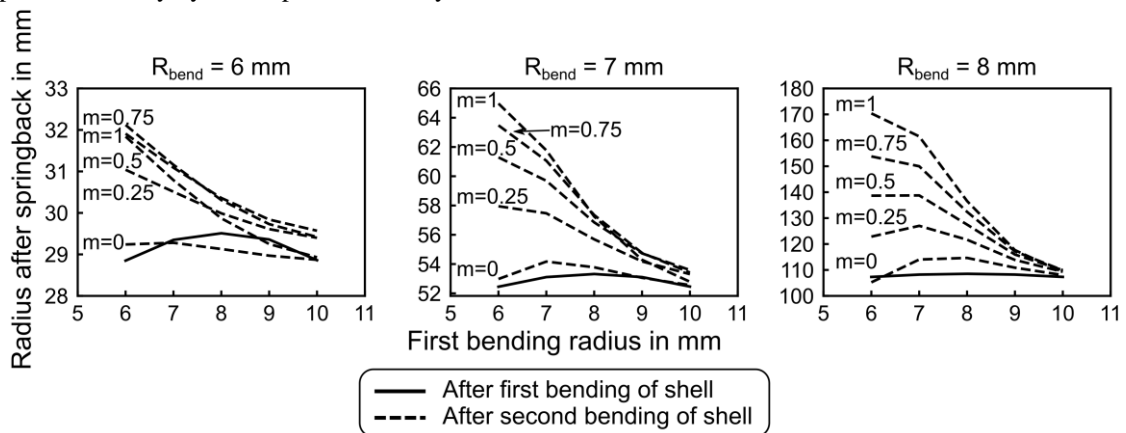


Fig. 5: Shell radii after elastic springback after first and second bending of the shell for the different m -values calculated using semi-analytical model.

4 Investigation of bistability using the extended semi-analytical model

4.1 Influence of bending radii combinations for measured material properties

The influence of bending radii combination on the bistability of metallic shells is investigated for the different materials presented in Chapter 3. The shell thickness is equal to 0.2 mm. For steel 1.1274 the study was done using bending radii from 4 to 12 mm with a step size of 0.1 mm. The results are depicted in Fig. 6. For steel 1.4310 the study was done using bending radii from 4 to 17 mm with a step size of 0.1 mm. The results are depicted in Fig. 7. As can be seen, with decreasing yield strength of the material, the range of radii combinations that lead to bistability increases.

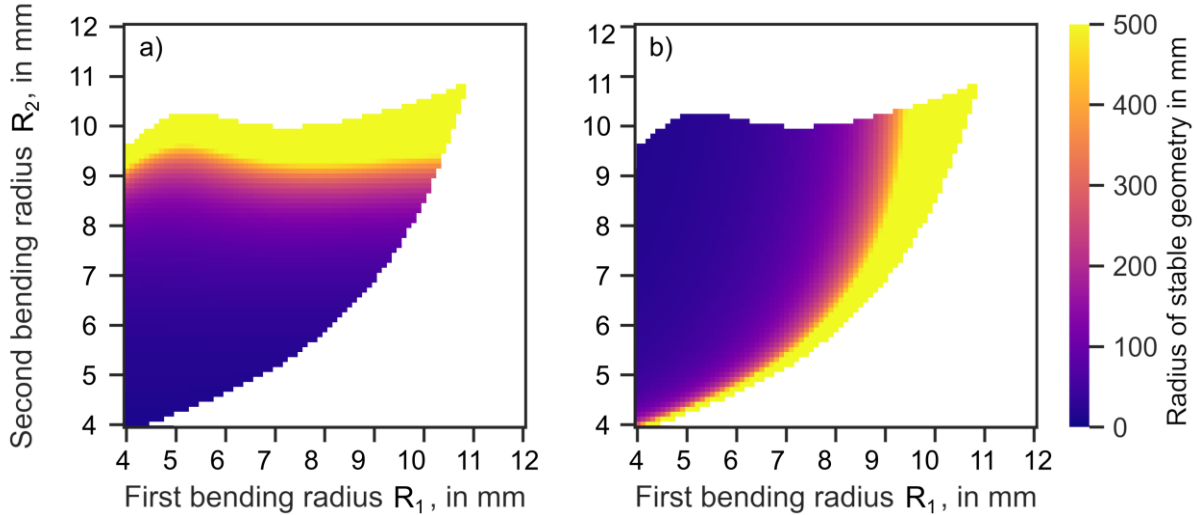


Fig. 6: Bistability and radii of a) first and b) second stable geometry for steel 1.1274 depending on different bending radii combinations.

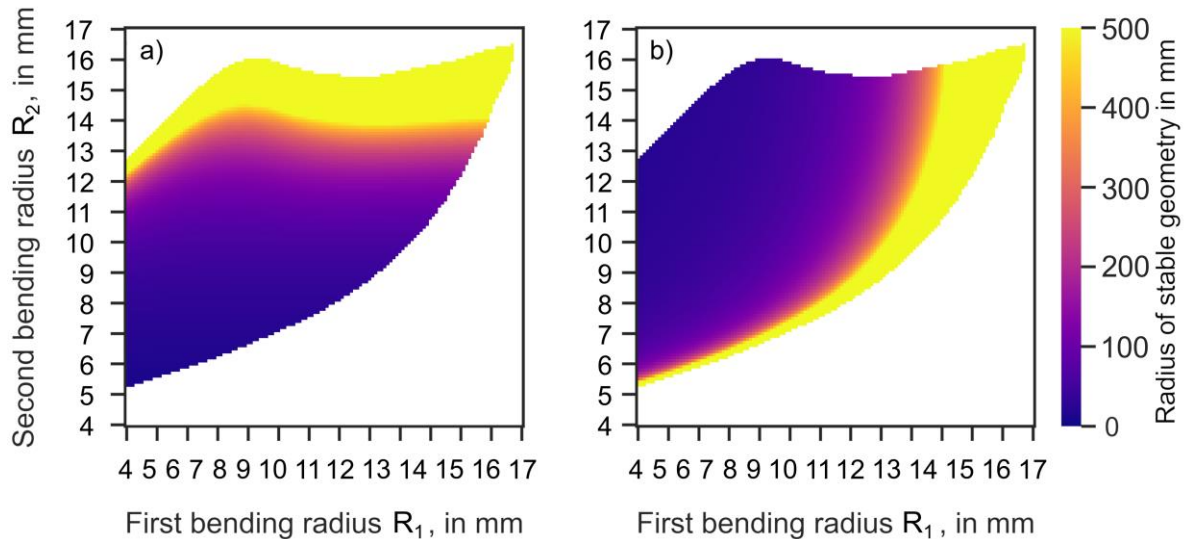


Fig. 7: Bistability and radii of a) first and b) second stable geometry for steel 1.4310 depending on different bending radii combinations.

4.2 Influence of yield stress disturbances on bistability

In addition to the calculations with the material values actually measured, parameter studies were also carried out for individually varied characteristic values.

The dependency of stable geometry radii regarding fluctuations of yield strength (± 200 MPa) of the shell is presented in Fig. 8 and Fig. 9 for the materials 1.1274 and 1.4310, respectively. The analysis was done for the bending radii combinations 6–6 mm, 7–7 mm, 8–8 mm, 9–9 mm and 10–10 mm for steel 1.1274 and 8–8 mm, 9–9 mm, 10–10 mm, 11–11 mm, 12–12 mm for steel 1.4310, respectively.

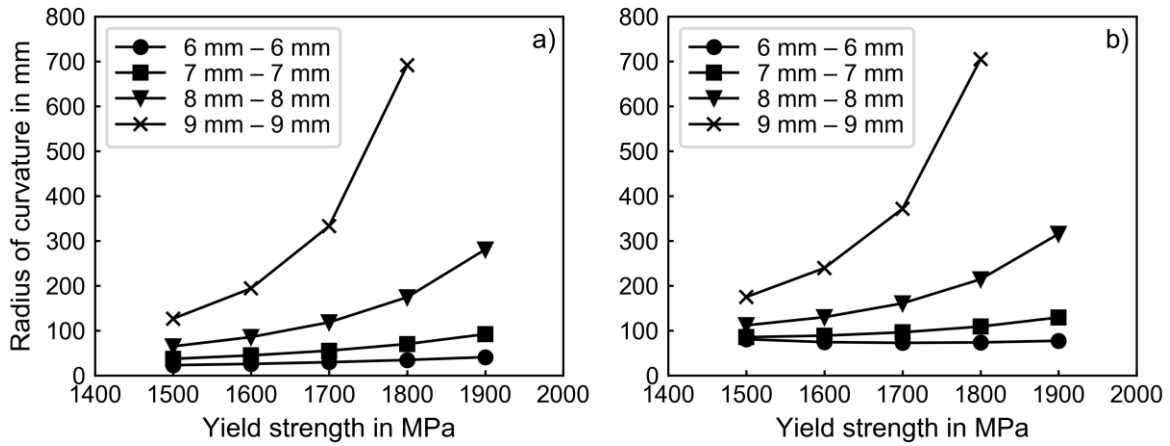


Fig. 8: Dependence of a) first and b) second stable state geometries on yield strength fluctuations for steel 1.1274.

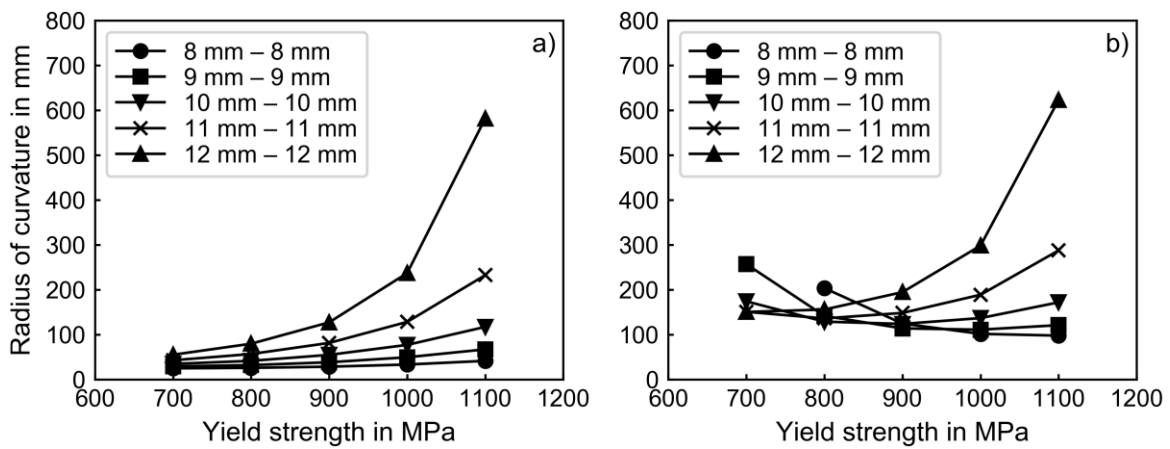


Fig. 9: Dependence of a) first and b) second stable state geometries on yield strength fluctuations for steel 1.4310.

It can be seen for both materials that with increasing bending radii the influence of yield strength fluctuation increases rapidly. This can be explained by the fact, that larger bending radius introduces smaller residual stresses in the shell, and even small changes of the yield strength leads to high deviations of stable geometry radii.

4.3 Influence of shell thickness disturbances on bistability

The dependency of stable geometry radii regarding fluctuations of the shell thickness (± 0.01 mm) is presented in Fig. 10 and Fig. 11 for the materials 1.1274 and 1.4310, respectively. The analysis was done for the same bending radii as in chapter 4.2. The properties of the materials were taken from Table 1.

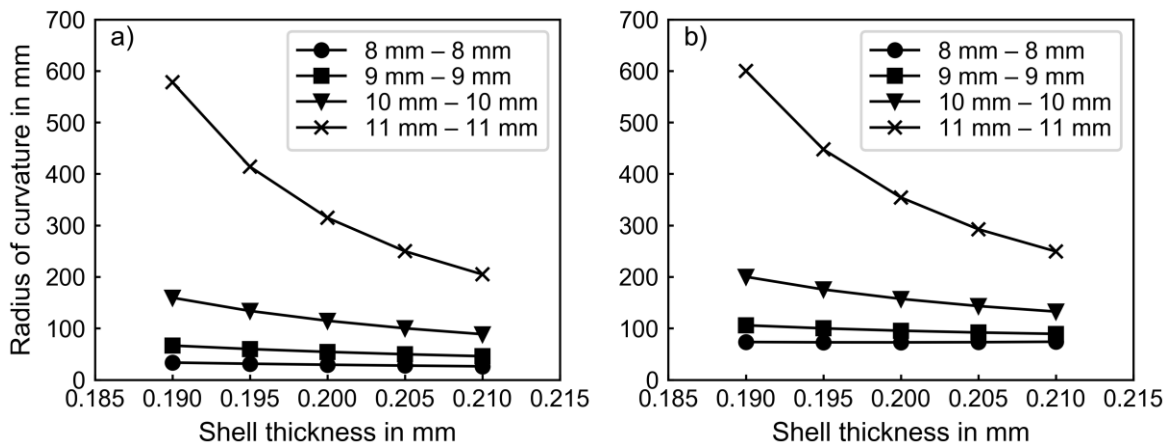


Fig. 10: Dependence of a) first and b) second stable state geometries on shell thickness fluctuations for steel 1.1274.

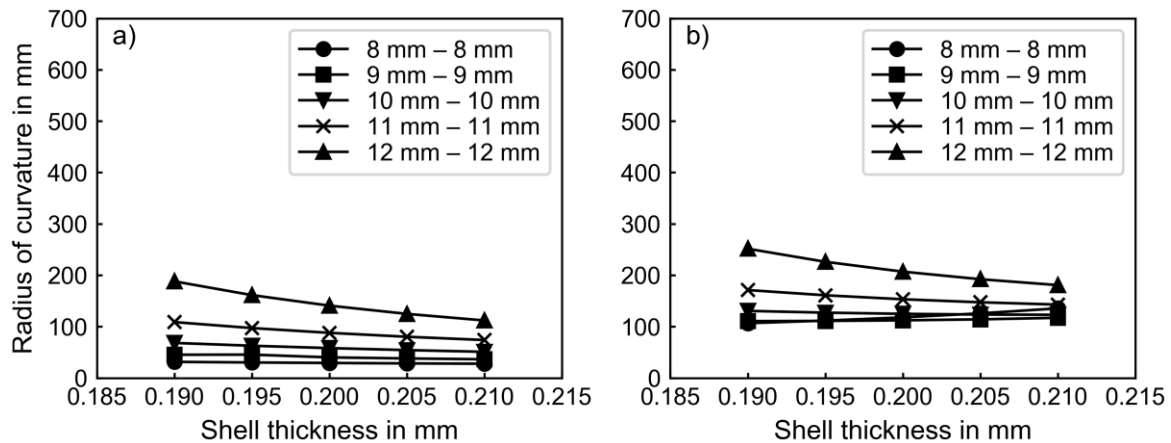


Fig. 11: Dependence of a) first and b) second stable state geometries on shell thickness fluctuations for steel 1.4310.

As in Chapter 4.2 it can be stated for both materials that with increasing bending radii the influence of shell thickness fluctuations increases significantly. The shell thickness has influence on the residual stress distribution as well as on the global stiffness of the shell and by that on the springback behavior.

5 Conclusions

The analysis of influences of production parameters as well as fluctuation of material properties on bistability of metallic shells was performed via a combined isotropic/kinematic hardening model.

The following conclusions can be made for the variation of the bending radii combination:

- Increasing of the first bending radius at a constant second bending radius leads to an increasing first stable geometry radius as well as a decreasing second stable geometry radius.
- Increasing of the second bending radius at constant first one has the opposite effect.
- Reducing the yield strength of the material increases the number of possible bending radii combinations that leads to bistability.
- Also smaller yield strength of the material allows for obtaining the bistable properties of the metallic shell by bending around higher bending radii, which reduces the number of required incremental bending operations.

The analysis of the influence of the yield strength fluctuations provides the following conclusions:

- Increasing of the yield stress of the shell while keeping other parameters constant (Young's modulus, shell thickness, bending radii combination) leads to an increase of the radii of both stable geometries for steel 1.1274.
- Nevertheless, the influence of the yield strength fluctuation on the second stable geometry is not so pronounced for steel 1.4310. For small bending radii (8 mm – 8 mm and 9 mm – 9 mm) the second stable geometry decreases with increase of yield strength. For higher bending radii combinations the radius of second stable geometry increases with an increase of the yield strength.
- Nonetheless, the influence of yield strength fluctuation is significantly higher with increase of the bending radii value. The larger the bending radius, the greater the deviation of the stable geometry.

From the investigation of the shell thickness fluctuations the following conclusions are made:

- The increase of the shell thickness while keeping constant other parameters (Young's modulus, yield strength, bending radii combination) leads to a decrease of the radii of the first and second stable geometry for steel 1.1274.
- Nevertheless, for steel 1.4310 the effect of thickness fluctuations on the radius of second stable geometry is not so straightforward. For the small bending radii (8 mm – 8 mm and 9 mm – 9 mm) the second stable geometry increases with higher thickness. For higher bending radii combinations, the second stable geometry radius starts to decrease with increase of the shell thickness.
- The fluctuation of the shell thickness has much more noticeable effect on the stable state geometries at higher bending radii combinations.

Overall, the new model allows the estimation and calculation of the influence of different shell and material properties. This allows even tighter requirements to be placed on the semi-finished product used and deviations between experiments (as shown in [3,4]) and the simulations can be better isolated. This enables the reliable production of bistable shells.

6 Acknowledgments

The authors thank the Deutsche Forschungsgemeinschaft (DFG, German Research Foundation) for funding within the priority program SPP 2013 “The utilization of residual stresses induced by metal forming” (project HI 790/57-1, № 374688658). Moreover, the authors like to thank Mrs. Shaoni Li for her support.

7 References

- [1] Pellegrino, S (2001) *Deployable Structures*; Springer: Wien, Austria.
- [2] Kebabze, E, Guest, S, Pellegrino, S (2004) Bistable prestressed shell structures. *Int. J. Solids Struct.* doi.org/10.1016/j.ijsolstr.2004.01.028
- [3] Pavliuchenko, P, Teller, M, Grüber, M, Bremen, T, Hirt, G (2019) Production of bistable fully closed metallic shells by introducing residual stresses during bending processes. *Prod. Eng. Res. Dev.* doi.org/10.1007/s11740-019-00875-6
- [4] Galletly, D, Guest, S (2004) Bistable composite slit tubes. I. A beam model. *Int. J. Solids Struct.* doi.org/10.1016/j.ijsolstr.2004.02.036.
- [5] Galletly, D, Guest, S (2004) Bistable composite slit tubes. II. A shell model. *Int. J. Solids Struct.* doi.org/10.1016/j.ijsolstr.2004.02.037.
- [6] He, X (2011) Bi-stable character of laminated cylindrical shells. *Proc. Eng.* doi.org/10.1016/j.proeng.2011.07.077.
- [7] Pavliuchenko, P, Teller, M, Grüber, M, Hirt, G (2019) A Semianalytical Model for the Determination of Bistability and Curvature of Metallic Cylindrical Shells. *Journal of Manufacturing and Materials Processing.* doi.org/10.3390/jmmp3010022
- [8] Crisfield, M (1997) *Non-Linear Finite Element Analysis of Solids and Structures, Volume 2: Advanced Topics*; Wiley: Hoboken, NJ, USA.
- [9] Patel, S, Lal, R, Dwivedi, J, Singh, V (2013) Springback analysis in shell metal forming using modified Ludwik stress-strain relation. *ISRN Mechanical Engineering* (2013), 1–11